Emission Mössbauer spectroscopy in the Co-O system under high oxygen pressure

K. Ruebenbauer and U.D. Wdowik

Mössbauer Spectroscopy Division, Institute of Physics, Pedagogical University
PL-30-084 Cracow, ul. Podchorążych 2, Poland
E-mail: sfrueben@cyf-kr.edu.pl

Short title: **Mössbauer spectroscopy in Co-O system**

Keywords: A. oxides, **C.** Mössbauer spectroscopy, **D.** diffusion
PACS Nos.: 61.72.-y, 33.45.+x, 66.30.Jt

Abstract

Results obtained by means of the emission Mössbauer spectroscopy in CoO and Co_3O_4 systems kept under relatively high oxygen pressure (air close to the normal pressure) are reported. Broadening of the 14.4-keV ^{57}Fe Mössbauer line due to the diffusion of iron atoms in CoO has been investigated in the temperature range between 1275 K and 1450 K. The excess of the linewidth caused by diffusive motions obeys the Arrhenius law with the activation energy of 1.86(8) eV. Mixed valence oxide Co_3O_4 was examined vs. temperature. Measurements were performed from the room temperature till 1073 K. Tetrahedrally coordinated iron impurities in the Co_3O_4 host lattice are in the high spin trivalent state despite the parent Co is divalent. The anharmonic contribution to the lattice vibrations at high temperatures was observed and analyzed for CoO and Co_3O_4 both.

1 Introduction

Cobaltous oxide, CoO, has been extensively studied by the Mössbauer spectroscopy in the last few decades. Most of these studies have been focused on the explanation of the origin of nucleogenic-iron aliovalent charge states, the latter being present in the host matrix. Generally, CoO has been investigated under low oxygen pressure as long as the emission Mössbauer spectroscopy is concerned. For a review see Refs [1, 2] and references listed therein.

Cobalt (II) oxide is a metal-deficient, NaCl-structured oxide, which exhibits p-type semiconducting properties at high temperatures. The important point defects are vacancies associated with the cation deficiency. A concentration of the cationic vacancies is governed by the oxygen partial pressure. CoO is stable either in the very high temperatures or in the lower temperatures provided the oxygen pressure under the sample is sufficiently low in the latter case. CoO can be oxidized to mixed valence oxide Co_3O_4 at lower temperatures and under high oxygen pressure [3].

Crystallographic unit cell of Co_3O_4 is shown in Fig. 1. Co_3O_4 has a normal spinel structure, and hence the chemical unit cell is cubic and it contains 56 atoms, i.e., it contains eight formal molecules of the compound. There are 32 anions distributed evenly between octahedral and tetrahedral units. Anions are divalent, while cations are either divalent or trivalent. Therefore, the chemical unit cell of the normal spinel contains 4 divalent cations in the tetrahedral T1 sites constituting FCC sub-lattice, 4 divalent cations in the tetrahedral T2 sites, and 16 trivalent cations in the octahedral O sites. Hence, the chemical formula of Co_3O_4 can be written as $[Co^{2+}(t)][Co^{3+}(o)]_2[O^{2-}]_4$ [4-7]. Tetrahedrally coordinated divalent Co ions (by oxygen anions) become antiferromagnetically ordered at about 40 K [4, 7]. They are ordered in such a way, that spins located in the T1 sites point in one of the main directions of the unit cell, while spins located in the T2 sites point in the opposite direction. Trivalent cobalt ions located in the octahedral sites are diamagnetic due to the crystal field splitting of $3d^6$ orbitals in the octahedral crystal field. The interaction of the electrons with the crystal field results in pairing of the electrons in the lower triplet t_{2g} levels leading to the diamagnetic $^1A_1$ state [4]. The cations on different sub-lattices differ in their electric and magnetic hyperfine interactions. Since the Co_3O_4 compound is paramagnetic either at room temperature (RT) or at elevated temperatures, no hyperfine magnetic splitting is observed in Mössbauer spectra measured under such thermal conditions. All cations in the tetrahedral sites experience such symmetry that second order and rank traceless symmetric tensors vanish on these sites. The electric field gradient tensor has the property of the above tensors and hence, the electric quadrupole interaction vanishes at these sites. T1 sites become equivalent to T2 sites provided the oxygen parameter equals $u = 3/8$. On the other hand, cations in the octahedral sites experience axially symmetric electric field gradient (EFG) tensor oriented along one of the cell diagonals. Sites with all eight possible orientations are equally populated. Due to the fact that the interaction with EFG is insensitive to the inversion operation, one can reduce the above eight possible states to the four states. Hence, there is an axially symmetric EFG at the octahedral sites with the main axis pointing at one of the four <111> directions, see Fig. 1, unless the condition $u = 3/8$ is satisfied. Anions split into two equally abundant populations except for $u = 3/8$. One of these populations belongs to the tetrahedral T units, while the other one to the octahedral O units. In addition, cations, e.g. substitutional isolated nucleogenic irons on different sub-lattices reveal different isomer shifts. Therefore, the Mössbauer spectra of the

paramagnetic phase should consist of a single resonance line arising from the cations on the tetrahedral sites provided T1 and T2 sites remain indistinguishable one from another, and a doublet originating from those located on the octahedral sites.

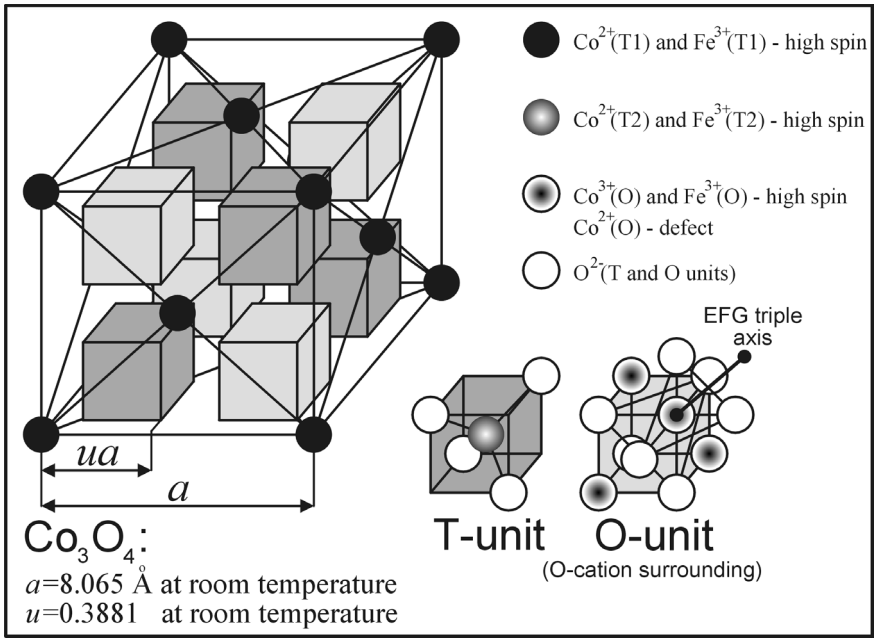

Fig. 1. Structure of the normal spinel Co_3O_4 compound.

The present paper deals with the emission Mössbauer spectroscopy, a microscopic method applied to look upon diffusivity in cobalt oxide. Behavior of the diluted iron impurities in Co_3O_4 and CoO host matrices is discussed, and the dynamical properties of both compound lattices are reported as well.

2 Experimental

The Mössbauer sources of (^{57}Co)CoO and (^{57}Co)Co_3O_4 were prepared using CoO single crystal. Details of the sample preparation procedure can be found elsewhere [1]. The uniform distribution of the ^{57}Co activity in the sample under investigation corresponded to the concentration of the radioactive cobalt and nucleogenic iron at the level of 40-at. ppm, altogether. The Co_3O_4 source was obtained by oxidizing (^{57}Co)CoO in air at 1123 K for about 6 hours. Subsequently the sample was cooled down to RT.

Mössbauer spectra of (^{57}Co)CoO were measured vs. temperature and sample orientation on freshly prepared single crystalline source. A temperature range from 1253 K to 1450 K was covered. Measurements were performed in air and for the beam outgoing in the [110] plane along various directions. Since no measurable directional dependence of the emitted radiation was detected, results obtained for the beam parallel to the <111> direction are reported solely. The lack of the directional dependence of the diffusion driven line broadening is explained by the build-up of the significant mosaic at very high temperatures leading to the effective poly-crystallization of the sample.

Mössbauer spectra of (^{57}Co)Co_3O_4 were measured as a function of the increasing temperature. Measurements were carried out in air and for the temperatures ranging from

RT to 1073 K. Room temperature spectra were obtained after having the sample cooled down from various elevated temperatures.

All spectra were recorded and evaluated using hardware equipment and software described in Refs [1, 8]. All spectra were evaluated within the transmission integral approximation, and hence all linewidths reported are the widths observed within the source. The air pressure was close to the normal (atmospheric) pressure i.e. the sample remained always under the ambient atmospheric pressure.

3 Results

3.1 CoO region

The set of high temperature Mössbauer spectra of CoO is shown in Fig. 2. Compared to the unbroadened spectrum taken at 1253 K the remaining spectra are clearly broadened. A minimum linewidth of 0.21(1) mm/s was measured at 1253 K. A temperature dependence of the source linewidth is plotted in Fig. 3. A comparision with linewidths obtained for low oxygen pressure (ca. 10^{-4} atm) [1] was made (see the lower curve in Fig. 3). One can see that the oxygen partial pressure controls a diffusion rate of the isolated iron impurity, as it controls the concentration of the cation vacancies. Diffusional broadening strongly depends not only upon the temperature, but also upon the concentration of Co vacancies. It should be noted that it was difficult to obtain data of sufficient quality above 1450 K due to large broadening of the spectrum and simultaneous decrease of the recoilless fraction at very high temperatures as well.

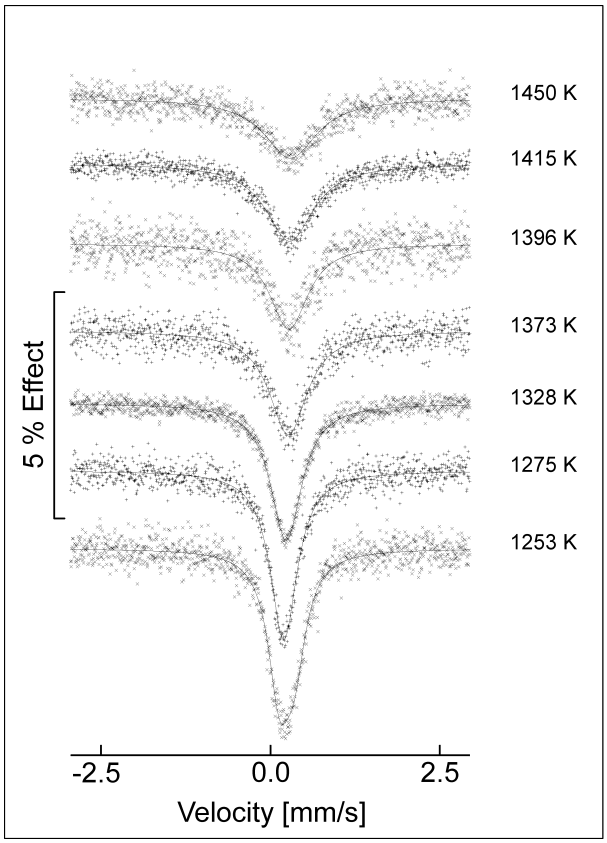

Fig. 2. Mössbauer spectra of (^{57}Co)CoO shown vs. temperature.

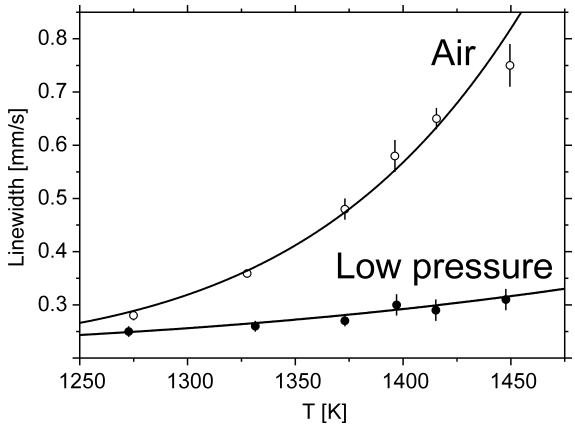

Fig. 3. Diffusional broadening of the resonance line vs. temperature for CoO. The upper and the lower curves correspond to the CoO spectra measured at high and low oxygen pressures, respectively.

Iron produced by the decay of ^{57}Co was found to be in the trivalent high spin-state. A temperature dependence of the isomer shift (S), i.e., a spectrum shift corrected for a second order Doppler effect, the latter being described by the Dulong-Petit rule [1], is plotted in Fig. 4. A Dulong-Petit rule gives for the Mössbauer transition in question shift amounting to 7.31×10^{-4} mm/(sK) for 1 K difference in temperature between source and absorber. A comparison with the isomer shifts obtained for CoO investigated at low oxygen pressure was made [1] (see the lower curve in Fig. 4). A polynomial fit has been applied to both data sets as described previously [1]. Isomer shifts are referred to the metallic iron of the natural isotopic abundance kept at RT. One can conclude that the daughter iron is located substitutionally at the host cobalt sub-lattice. The inset of Fig. 4 shows the mobility ratios α vs. temperature as obtained for high and low oxygen pressure, respectively. The mobility ratio has been discussed in more detail in Ref. [1].

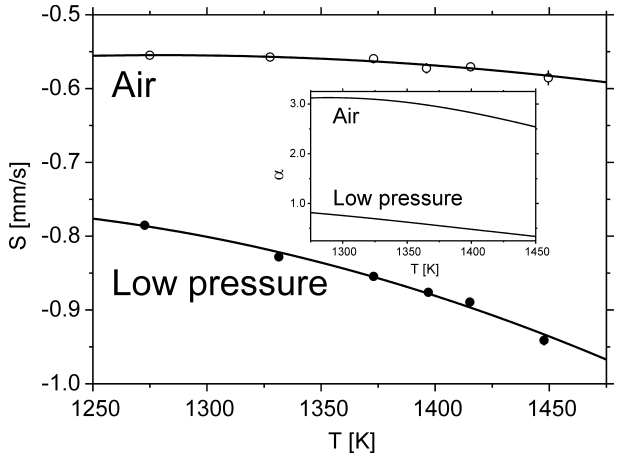

Fig. 4. Isomer shift of CoO vs. temperature for high and low oxygen pressures. The inset shows the mobility ratio vs. temperature for high and low oxygen pressure, respectively. The mobility ratio is a dimensionless parameter.

3.2 Co_3O_4 region

Mössbauer spectra obtained for the decay product of the ^{57}Co in Co_3O_4 are shown in Fig. 5. Since the effects of the radioactive decay are not sufficient to remove the nucleogenic Fe from the initial Co lattice position, the hyperfine parameters of the Mössbauer spectra could be used to determine and verify the distribution of Co over the cobalt sub-lattices. A daughter Fe was found to occupy both tetrahedral and octahedral Co lattice sites. Similar results have been obtained previously by Mössbauer spectroscopy [6, 7], however these earlier experiments were performed in the temperature range not exceeding 595 K, and they were mainly devoted to the study of the magnetic properties of Co_3O_4 [7]. Tetrahedrally located Fe is in the high spin trivalent state, even though the parent Co in the tetrahedral site is divalent. It is well known that the charge-state of the daughter Fe produced by the Co decay is not always the same as that of the initial cobalt [6-8]. Cobalt monoxide is an example, where the initial divalent Co decays to both Fe^{2+} and Fe^{3+} valence states [1]. Mössbauer spectra of ^{57}Fe in Co_3O_4 shown in Fig. 5 consist of a symmetrical doublet and a singlet. A doublet originates from the decay of the Co^{3+} ion to the Fe^{3+} ion at the octahedral site having trigonal symmetry, while the singlet arises from the Co^{2+} decaying to the Fe^{3+} at the tetrahedral site being equivalent to the cubic sites for the electric field gradient tensor. The RT isomer shifts of the T-site line [-0.336(2) mm/s] and O-site doublet [-0.416(5) mm/s] are typical for the trivalent Fe located at the tetra- and octahedral normal spinel sites [6, 7].

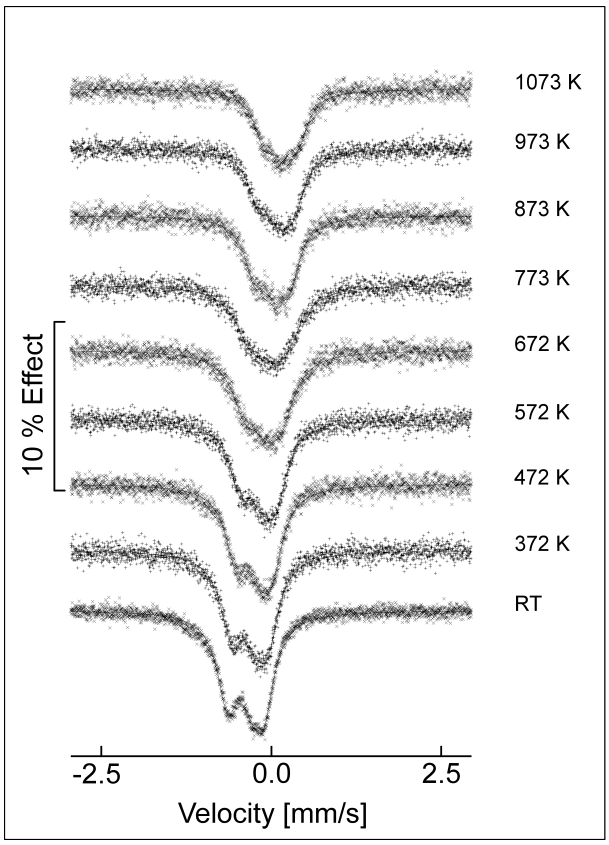

Fig. 5. Mössbauer spectra of (^{57}Co)Co_3O_4 shown vs. temperature.

A temperature dependence of isomer shifts corresponding to tetrahedral and octahedral sites is plotted in Fig. 6. A linear fit to both data sets has been applied. Due to the fact that

the oxygen parameter is larger than 3/8 an electric field gradient was observed at the octahedral sites. No significant changes of the quadrupole splitting were seen, as a function of the temperature. The last statement applies to the range RT till 873 K. The mean value of the quadrupole splitting equals 0.534(1) mm/s and it stays in good agreement with the values of 0.535 mm/s and 0.52 mm/s reported in Refs [6, 7], respectively. The quadrupole splitting tends to diminish above ca. 973 K, i.e., in the temperature region where the mixed valence oxide Co_3O_4 starts to convert to the CoO phase.

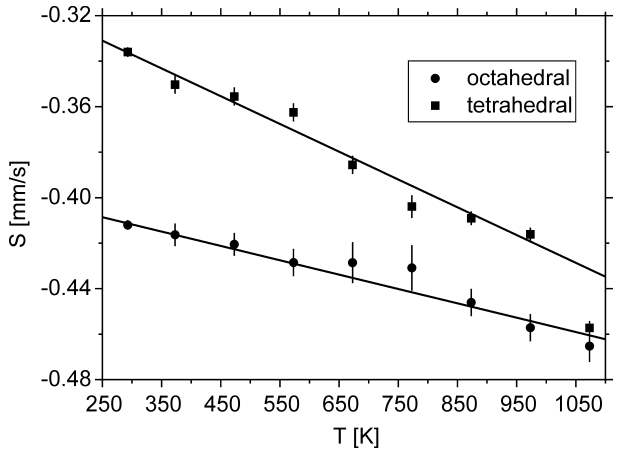

Fig. 6. Isomer shifts of tetrahedrally and octahedrally coordinated iron impurity in Co_3O_4. The upper and the lower curve are due to the T and O sites, respectively.

Mössbauer data allow determination of relative contributions of the O-site doublet and the T-site singlet to the emission spectrum. The values obtained are 33(2)% and 67(2)% for singlet and doublet, respectively. They correspond to the expected occupancies by the cobalt atoms, i.e., 1/3 of the cations located in the tetrahedral sites, and remaining 2/3 cations residing in the octahedral sites. Hence, the recoilless fractions remain the same for all sites at all temperatures, and they vary with the temperature in the same manner.

4 Discussion

A temperature dependence of the iron isomer shift in CoO investigated under low oxygen pressure has been previously discussed, and the theoretical background has been elaborated as well [1]. In the case of CoO examined at high oxygen pressure (air) the same theoretical approach could be used. The isomer shift behavior at high temperatures has been described by the mobility ratio $\alpha = (v_p\sigma_p)/(v_e\sigma_e)$ of the respective carriers, i.e., holes and electrons denoted as *p* and *e*, respectively. The carrier velocity v depends upon temperature and defect (vacancy) concentration, the latter being dependent on the oxygen pressure as well. Respective cross-sections for absorption by the iron ion, σ, were assumed to be constant in the system under consideration. Polynomial fits shown in Fig. 4 yielded parameters, which could be used to calculate the mobility ratio vs. temperature, the latter shown in Fig. 4 as inset. Positive carriers are more mobile as compared to the electrons at high oxygen pressure due to the increased defect concentration. Apparent reduction of the electron mobility is associated with the enhanced electron scattering on the point defects, i.e., on the vacancies. On the other hand, electron mobility increases with the increasing temperature as CoO exhibits still properties of a typical semi-conductor even at very high temperatures.

Diffusional broadening of the Mössbauer resonance line [9] can be used to determine the temperature dependence of the diffusion coefficient D [10-12]. In order to calculate D vs. temperature one needs to make some assumptions about the microscopic mechanism of diffusion. Since CoO is of the NaCl-type, a simple mono-vacancy mechanism in the FCC lattice was considered. Additionally, the following approximations have been made: the source is resonantly thin having the intrinsic line shape described by the Lorentzian profile. A broadening is small enough to neglect non-Lorentzian contribution to the emission profile [10]. Moreover, the Mössbauer atom jumps to the nearest neighbor sites in the FCC lattice and the uncorrelated nearest neighbor jumps are considered as the uncorrelated events leading to the diffusion [10]. Under such circumstances a diffusion coefficient of the iron impurity can be expressed as follows [10]:

$$D = \tfrac{1}{12}\omega a^2 \ . \tag{1}$$

Here the symbol ω denotes the average jump frequency of the iron impurity and the symbol a stands for the lattice constant (a=4.2511 Å at RT). The lattice parameter a was approximated by the temperature independent RT value, as the changes due to the varying temperature and stoichiometry are small enough to be neglected. A frequency ω satisfies the following relationship $\omega = (\Delta\Gamma\, q)/\langle\gamma\rangle$, where the symbol $\Delta\Gamma$ stands for the excess source linewidth due to the diffusional motions, and q denotes the wave number of the emitted 14.41-keV Mössbauer radiation (7.31 Å^{-1}) to a very good approximation. A geometrical factor $\langle\gamma\rangle$ for the random sample approximation and for the uncorrelated jumps to the nearest neighbor positions in the FCC lattice satisfies the following relationship [10-12]:

$$\langle\gamma\rangle = 1 - \left(\frac{4}{3\pi}\right)\int_0^{\pi/4} d\phi \int_0^{\pi/2} d\beta \sin(\beta)\left[\cos\psi_1\cos\psi_2 + \cos\psi_1\cos\psi_3 + \cos\psi_2\cos\psi_3\right] \ . \tag{2}$$

The phase angles take on the following forms:

$$\begin{aligned} \psi_1 &= \tfrac{1}{2} aq \sin\beta\cos\phi \,, \\ \psi_2 &= \tfrac{1}{2} aq \sin\beta\sin\phi \,, \\ \psi_3 &= \tfrac{1}{2} aq \cos\beta \,. \end{aligned} \tag{3}$$

Here the symbols β and ϕ stand for the polar and azimuthal angles of the wave-vector transfer to the system expressed in the main crystallographic axes, respectively. A diffusion coefficient calculated using above equations follows the Arrhenius law as shown in Fig. 7. The activation energy of 1.86(8) eV was obtained. It stays in fair agreement with the values obtained by a tracer-sectioning technique, i.e., 1.56 eV in the case of ^{59}Fe [13, 14], 1.52 eV in the case of ^{55}Fe [13, 14] (see Fig. 7) and 1.4 eV [15]. Since the directional dependence of the line broadening was hardly observed, the microscopic diffusion mechanism, i.e., the elementary jump vectors and frequencies could not be quantitatively determined. However, the measurements performed at the reduced oxygen partial pressure (see Fig. 3 for details) suggest, that impurities diffuse through the cobalt sub-lattice via the mono-vacancy mechanism. Cobaltous oxide goes to more stoichiometric form under reduced oxygen partial pressure due to the lower vacancy

concentration. Diffusion jumps are assumed to lead Fe impurity to the vacancies located as the nearest neighbors. A small number of vacancies in the neighborhood results in the very small diffusional line broadening for the sample examined under reduced pressure, in contrast to measurements performed in air (compare the lower and upper curves of Fig. 3). Hence, our results support vacancy migration mechanism for cobalt/iron diffusion in CoO experimentally confirmed by a tracer technique [13, 14]. A vacancy mechanism of diffusion is characterized by the vastly different pre-exponential factors of the diffusion coefficient, the latter being dependent upon the oxygen pressure. Pre-exponential factors for CoO obtained for air and low oxygen pressure equal $2.0(9)\,\mathrm{x}\,10^{-2}$ cm^2/s and $2(1)\,\mathrm{x}\,10^{-3}$ cm^2/s, respectively. On the other hand, activation energy practically does not depend upon the sample stoichiometry i.e. it is independent of the oxygen pressure. Similar conclusions were reached by means of the tracer technique [13, 14]. Hence, one can write a diffusion coefficient in the form:

$$D = \omega_0 c_p a^2 \exp[-(U_0 + B_0)/(k_B T)] \ . \tag{4}$$

Here the symbol ω_0 denotes the average frequency of the Fe jump originating at any site and ending at one of the nearest neighbor sites - in the infinite temperature limit. The symbol c_p stands for the oxygen pressure dependent vacancy concentration in the same limit, U_0 stands for the vacancy creation energy, B_0 denotes the energy barrier for the above jump, k_B stands for the Boltzmann's constant, and finally T stands for the temperature. The last expression is valid provided the parameter c_p stays much lower than unity. It applies to the temperature region, where all vacancy clusters are already dissolved [1]. Actually our activation energy equals $U_0 + B_0$. It seems that all parameters of the equation (4) are very weakly dependent upon the temperature as otherwise one can expect some deviation from the Arrhenius law. Somewhat higher activation energy found by us in comparison with the tracer method is an indication that the diffusion along extended defects is faster than in the bulk. The Mössbauer spectroscopy as the microscopic method is practically insensitive to the extended defects in contrast to the macroscopic tracer method.

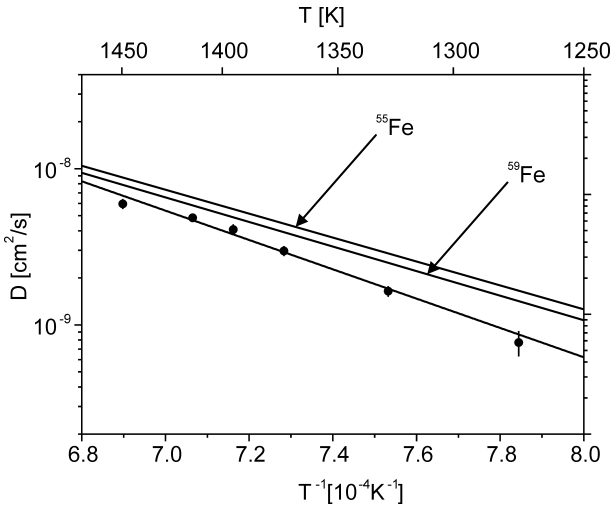

Fig. 7. Iron diffusion coefficient for CoO plotted in the Arrhenius coordinates.

The octahedral ion charge-state in Co_3O_4 remains unchanged after the radioactive decay, i.e., the parent Co^{3+} transforms to Fe^{3+}. Quite different behavior is observed for a daughter impurity created in the tetrahedral sites. Tetrahedrally coordinated daughter iron forms trivalent charge-state despite divalent state of the initial cobalt. A conversion of the nucleogenic iron to the trivalent ion occurs prior to the Mössbauer level formation. The electron is transferred to the octahedrally coordinated Co^{3+} converting it to the divalent Co having character of the isolated point defect. Hence, each of the iron impurities occupying tetrahedral position is accompanied by the divalent cobalt located in the octahedral site. It is likely that these Co^{2+} states become delocalized over all octahedral sites occupied by cobalt at higher temperatures, i.e., well above the magnetic transition temperature, contributing to the overall electric conductivity. Electron hopping mechanism is supposed to be responsible for such phenomenon. A schematic diagram of the process described above together with the expected electronic energy levels of cations is shown in Fig. 8.

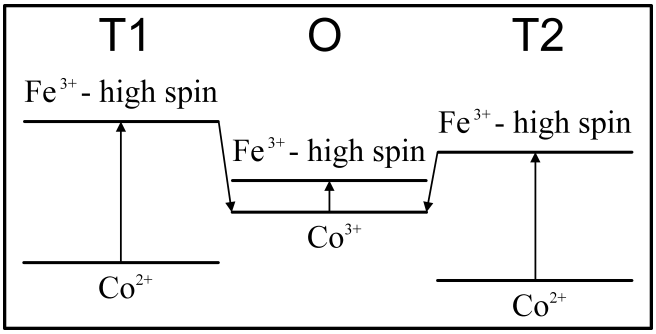

Fig. 8. Schematic diagram of the expected electronic energy levels for cations in Co_3O_4.

The isomer shift S of the diluted iron impurity located in tetrahedral sites is greater than the isomer shift of Fe in octahedral positions as can be seen in Fig. 6. Emission Mössbauer spectra measured above the magnetic transition temperature are composed of the doublet originating from the octahedral Fe and two closely related singlets coming from T1 and T2 sites (see Figs 1 and 5 for details). One can calculate appropriate distances to the nearest neighbors, i.e., to the anions from the cations located in respective sites (in the case of unperturbed lattice). One obtains the following distances:

$$d(\mathrm{T1}) = \sqrt{3}\,a\,(\tfrac{1}{2} - u)\ ,\ d(\mathrm{O} \to \mathrm{O}) = 2\,a\,(u - \tfrac{1}{4})\ ,$$
$$d(\mathrm{T2}) = \sqrt{3}\,a\,(u - \tfrac{1}{4})\ ,\ d(\mathrm{O} \to \mathrm{T}) = 2\,a\,(\tfrac{1}{2} - u)\ .$$

Here the symbol u denotes the oxygen parameter. The oxygen parameter has to satisfy the following condition $\frac{1}{4} < u < \frac{1}{2}$. One obtains the following distances for Co_3O_4 in the vicinity of RT, i.e., for u=0.3881 [4]:

d(T1) = 1.563 Å, d(T2) = 1.929 Å, $d(\mathrm{O} \to \mathrm{O})$ = 2.228 Å, and $d(\mathrm{O} \to \mathrm{T})$ = 1.805 Å.

In the case of Co_3O_4 T1 sites are more closely packed than T2 sites due to the oxygen parameter being greater than 3/8 (see Fig. 1). Hence, the Mössbauer spectrum originating from the resonantly thin source consists of two singlets giving 1/6 contribution each and a doublet giving 2/3 contribution provided recoilless fractions are the same for all sites. Hence, the resulting linewidth corresponding to the tetrahedral iron was observed to be greater than the linewidth of the doublet, i.e., 0.209(4) mm/s and 0.105(2) mm/s at RT,

respectively. A doublet is symmetrical as long as the recoilless fraction in the O-site is isotropic. No directional dependence of the intensities within the doublet components is expected under such circumstances even for the single crystal sample.

The isomer shifts of both components gradually decrease with increasing temperature as can be seen in Fig. 6. Electron density on the iron nucleus embedded in tetrahedral sites increases more rapidly as compared to the octahedral sites mainly due to the more closely packed arrangement of T-sites (see Fig. 1 and the appropriate distances for T and O sites listed above). Bonding properties of the tetrahedral surrounding are of more ionic character and account for the observed effect. A decrease of the isomer shift with the increasing temperature can be explained as the increase of the concentration of the quasi-free electrons with the increased temperature. Such explanation is consistent with the observed enhancement of the electrical conductivity at higher temperatures. It has to be stressed that the isomer shifts discussed here are already corrected for the trivial second order Doppler shift.

Fig. 9 shows a dependence of the recoilless fraction of the 14.4-keV γ radiation on the temperature. A temperature range covered extends from RT to 1073 K. A recoilless fraction at each temperature was normalized to the recoilless fraction at RT and used to define effective mean-squared displacement (MSD) as described in detail in Ref. [1]. A temperature dependence of MSD could be approximated in the following way [1]:

$$(-1/q^2)\ln(f/f_0) = a(T - T_N) + b\eta(T - T_A)(T - T_A)^2 \ . \tag{5}$$

All symbols have the same meaning as in Ref. [1]. A temperature T_A has been taken as 773 K. The harmonic approximation, i.e., the linear part of the curve plotted in Fig. 9 was used to determine an effective Mössbauer characteristic temperature θ_M [1]. This temperature θ_M equals 540(5) K. A recoilless fraction expressed as MSD does not follow a linear dependence on temperature above the temperature T_A. The deviation from linearity is related to the anharmonicity of lattice vibrations. The anharmonicity parameter b obtained from the data fit equals 8.4(4) x 10^{-8} Å^2/K^2. In the high temperature limit, i.e., for $T > T_A$ [1], the mean squared-displacement can be approximated by the relationship $AT + BT^3$ [16-19]. The above expression can be expanded around T_A to the second order approximation, leading to the high temperature limit of the equation (5) describing MSD provided $B = b/(3T_A)$. The latter parameter equals 3.6(2) x 10^{-11} Å^2/K^3.

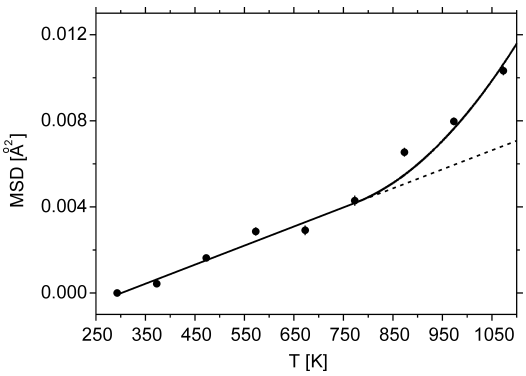

Fig. 9. Effective MSD plotted vs. temperature for Co_3O_4.

The same procedure was applied to evaluate recoilless fraction obtained for the CoO phase. The resulting curves are plotted in Fig. 10. A comparison with the data measured at low oxygen pressure was made. The linear parts of both MSD were assumed to be identical resulting in the characteristic temperature $\theta_M = 440(11)$ K [1]. The effective Mössbauer temperature determined by us is in accordance with values reported in Refs [20, 21]. In the case of CoO investigated in air, the anharmonicity parameter b equals 7.4(2) x 10^{-8} Å^2/K^2. One obtains $B = 7.40(7)$ x 10^{-11} Å^2/K^3 under assumption that T_A equals 923 K, i.e., that it is the same as under the low oxygen pressure [1]. The anharmonicity of the lattice vibrations is greater for CoO studied at high oxygen pressure than under low oxygen pressure (see Table 1 for comparison). The main reason for such a difference in the vibrational dynamics of iron impurity is due to the difference in concentration of cobalt vacancies, i.e., the sample stoichiometry governed by the oxygen pressure at high temperatures. The cobalt sub-lattice becomes softer at high oxygen pressure and substitutional Fe ions have more loose bonds to the host lattice.

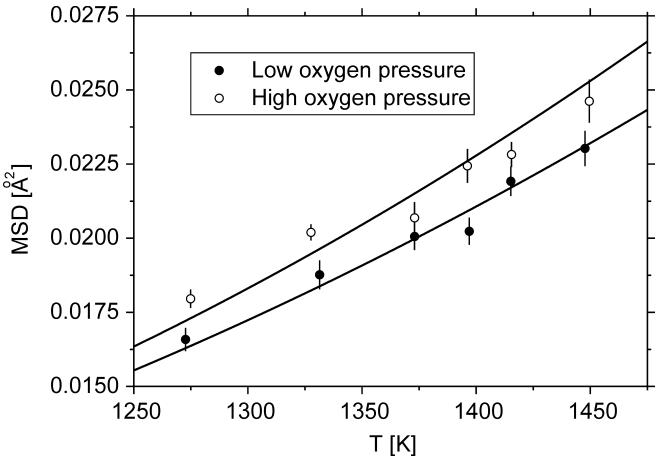

Fig. 10. Effective MSD plotted vs. temperature for CoO.

Table 1: Anharmonicity parameters for CoO.

Parameter	Low oxygen pressure	High oxygen pressure (air)
b [Å^2/K^2]	5.7(2) x 10^{-8}	7.4(2) x 10^{-8}
B [Å^2/K^3]	2.06(7) x 10^{-11}	7.40(7) x 10^{-11}

5 Conclusions

The principal results of the present work are as follows:

i) Cation diffusivity in CoO strongly depends upon the stoichiometry controlled by the oxygen pressure at high temperatures. Cationic diffusion is fast for non-stoichiometric CoO and it occurs via simple mono-vacancy mechanism. A diffusion coefficient of iron impurity obeys the Arrhenius law. The activation energy agrees reasonably well with the values determined by the tracer diffusion technique, albeit it is somewhat higher probably due to the fact that diffusion along extended defects remains unseen by the microscopic methods, i.e., by the Mössbauer spectroscopy.

ii) Structural defects, i.e., cation vacancies play an important role on the dynamical properties of the CoO lattice accounting for greater anharmonicity of the lattice vibrations, provided highly non-stoichiometric cobalt oxide is concerned. A vacancy concentration governs the mobility ratio of the electric charge carriers like electrons and holes as well, and the increased vacancy concentration is responsible for the increased mobility of the holes in comparison with the mobility of the electrons.

iii) In the case of Co_3O_4 the charge-state of iron following the electron-capture decay of the tetrahedrally coordinated divalent cobalt is always 3+ due to the electron transfer from the unstable Fe^{2+} to the octahedral Co^{3+}. The resulting divalent Co can be treated as delocalized state due to the electron hopping mechanism at the elevated temperatures.

iv) No traces of the trivalent cobalt oxide Co_2O_3 were found under oxidation conditions applied in this work. This oxide is easy to distinguish, as it exhibits spectrum characterized by a specific doublet.

v) Broadening found earlier under very low oxygen pressure was not confirmed, and it cannot be interpreted as due to the diffusive motion [22] of the atoms.

vi) Electric quadrupole interaction in Co_3O_4 is practically temperature independent. This is an indication that EFG is mainly of the lattice distortion origin, and that the oxygen parameter evolves very weakly with the varying temperature.

Acknowledgments

Dr. Artur Błachowski, Mössbauer Spectroscopy Division, Pedagogical University is thanked for his help in Mössbauer data collection.

References

[1] K. Ruebenbauer and U.D. Wdowik, J. Phys. Chem. Solids **65**, 1785 (2004). For *preprint* see: www.cyf-kr.edu.pl/~sfrueben/coo1.pdf

[2] P.P Seregin, F.S. Nasredinov, and L.N. Vasilev, phys. stat. solidi (a) **45**, 11 (1978).

[3] K. Przybylski and W.W. Smeltzer, J. Electrochem. Soc. **128**, 897 (1981).

[4] W.L. Roth, J. Phys. Chem. Solids **25**, 1 (1964).

[5] K. Miyatani, K. Kohn, H. Kamimura, and S. Iida, J. Phys. Soc. Jap. **21**, 464 (1966).

[6] C.D. Spencer and D. Schroeer, Phys. Rev. B **9**, 3658 (1974).

[7] W. Kündig, M. Kobelt, H. Appel, G. Constabaris, and R.H. Lindquist, J. Phys. Chem. Solids **30**, 819 (1969).

[8] U.D. Wdowik and K. Ruebenbauer, Phys. Rev. B **63**, 125101(8) (2001).

[9] K.S. Singwi and A. Sjölander, Phys. Rev. **120**, 1093 (1960).

[10] K. Ruebenbauer, Hyp. Int. **14**, 139 (1983).

[11] K. Ruebenbauer and B. Sepioł, Hyp. Int. **30**, 121 (1986).

[12] B. Miczko, K. Ruebenbauer, and B. Sepioł, Hyp. Int. **52**, 107 (1989).

[13] K. Hoshino and N.L. Peterson, J. Phys. Chem. Solids **45**, 963 (1984).

[14] K. Hoshino and N.L. Peterson, J. Phys. Chem. Solids **46**, 229 (1985).

[15] R. Dieckmann, Z. Phys. Chem. Neue Folge **107**, 189 (1977).

[16] K. Ruebenbauer and U.D. Wdowik, Phys. Rev. B **61**, 11416(2000).

[17] N.M. Butt and D.A. O'Connor, Proc. Phys. Soc. **90**, 247 (1967).

[18] C. Ghezzi, A. Merlini, and S. Pace, Nuovo Cim. B **64**, 103 (1969).

[19] G. Albanese, C. Ghezzi, A. Merlini, and S. Pace, Phys. Rev. B **5**, 1746 (1972).

[20] H.N. Ok and J.G. Mullen, Phys. Rev. **168**, 550 (1968).
[21] H.N. Ok and J.G. Mullen, Phys. Rev. **168**, 563 (1968).
[22] J. Fontcuberta, phys. stat. solidi (b) **139**, 379 (1987).